# Application of Wavelet Packet and S Transforms for Differential Protection of Power Transformer

**Waad Noori Taboor**
M.Sc student
Waad_nori@yahoo.com

**Dr. Adel Ahmed Obed**
Lecturer
adelrazan@yahoo.com

**Dr. Majed Abdul Nabi Alwan**
Lecturer
altimimee@yahoo.com

Department of Electrical Engineering, Basrah University

**ABSTRACT:**

The differential protection of power transformers appears to be more difficult than any type of protection for any other part or element in a power system. Such difficulties arise from the existence of the magnetizing inrush phenomenon. Therefore, it is necessary to recognize between inrush current and the current arise from internal faults. In this paper, two approaches based on wavelet packet transform (WPT) and S-transform (ST) are applied to recognize different types of currents following in the transformer. In WPT approach, the selection of optimal mother wavelet and the optimal number of resolution is carried out using minimum description length (MDL) criteria before taking the decision for the extraction features from the WPT tree. In ST approach, the spectral energy index and the standard deviation (STD) are calculated from the S-matrix obtained by discrete S-transform. The two approaches are tested for generating a trip signal and disconnecting the transformer supply experimentally using 1KVA, 220/110V, 50Hz, $\Delta / Y$ three-phase transformer. The experimental results show that the trip signal is initiated faster in WPT approach while the transformer is disconnected from the supply after a delay of 10-15msec in the two approaches due to computer interface and the relay circuit used.

**Keywords: differential protection, wavelet packet transform, S-transform, inrush and fault Currents recognition**

## استخدام تحويليتي ربطة المويجة وربطة المويجة المعدلة في الحماية التفاضلية لمحولة القدرة

**وعد نوري طابور**
**طالبة ماجستير**

**د. عادل احمد عبيد**
**مدرس**

**د. ماجد عبد النبي علوان**
**مدرس**

**الخلاصة:**

تبدو الحماية التفاضلية لمحولات القدرة أصعب من أية حماية لأي جزء أو عنصر في نظام القدرة. إن هذه الصعوبة تكمن من نشوء ظاهرة تيار التدفق المغناطيسي لحظة التشغيل. لذلك من الضروري التمييز بين تيار التدفق والتيارات الناشئة من تيارات الخطأ الداخلية. في هذا البحث تم استخدام طريقتين للتمييز بين تيار التدفق وتيارات الخطأ الداخلية اعتمادا على تحويله ربطة المويجة وتحويله ربطة المويجة المعدلة. في الطريقة الأولى تم اختيار المويجة الأم وأفضل مستوى حل باستخدام دالة الطول الأصغر قبل اتخاذ قرار استخلاص المعالم من شجرة تحويله المويجة. في الطريقة الثانية تم حساب دليل الطاقة الطيفية والانحراف القياسي من مصفوفة S التي حسبت من تحويله ربطة المويجة المعدلة. اختبرت كلا الطريقتين لتوليد إشارة عزل المحولة من المصدر عمليا باستخدام محولة ثلاثية الطور 1KVA, 220/110V, 50Hz $\Delta / Y$. أظهرت النتائج العملية بأن إشارة العزل تتولد أسرع في الطريقة الأولى بينما تنعزل المحولة عن المصدر بعد تأخير زمني من 10-15 ملي ثانية في كلا الطريقتين بسبب توصيلة الحاسبة ودائرة المرحل المستخدمة.

**الكلمات المفتاحية: الحماية التفاضلية، تحويله ربطة المويجة، تحويله S، تمييز تيارات الخطأ وتيارات التدفق.**

## 1- INTRODUCTION:

The protection of power transformer has been always in a challenge due to the problem of rapid discriminating between the inrush and internal fault currents. A possibility for false tripping of differential relay may be caused by the magnetizing inrush current during energization. Such wrong-operation of differential relays can affect both reliability and stability of the whole power system [S. A. Saleh, et. al., 2005].

The conventional methods use the second harmonic components to restrain operation of the differential relay during magnetizing inrush conditions. The main idea of the harmonic restraint differential relays is to extract the fundamental, the second and sometimes the fifth harmonics and to compare the ratio of the second and fifth harmonics with the fundamental to predefined threshold value. However, sometimes, the magnitude of second harmonic components in the internal fault current can be close to or greater than the magnitude of inrush currents. This may be due to saturation and the new low-loss amorphous core material in modern power transformer [B. A. Sykes, et., al., 1972 and M. R. Zaman, 1996].

The previous methods on power transformer protection include other approaches, among these approaches; calculation of transformer inductance during saturation, artificial neural network (ANN), flux and voltage restraints and fuzzy logic [L. D. Periz, et., al., 1994, A. Wiszniewski, et., al., 1995, M. R. Zaman, 1996, A. L. Oville, et., al., 2001, M. C. Shin, et., al., 2003, H. Khorashadi, 2006 ].

Recently, signal processing has been reported on use of time frequency localization for current signal recognition. Wavelet (WL) decomposition is ideal for studying transient signals and obtaining a much better current characterization and a more reliable recognition. It allows the decomposition of the signal into different levels of resolution. The mother wavelet function is dilated at low Frequencies and compressed at high frequencies so that large windows are used to obtain the low frequency components of the signal, while small windows reflect discontinuities. Therefore, from small windows, a certain features can be extracted to recognize between inrush and internal fault currents [S. A. Saleh, et. al., 2005, A. Rahmati, 2010, S. A. Saleh, et. al., 2010]. In WL analysis, a proper mother wavelet function and a level of decomposition should be chosen which are sometimes difficult, thereby the computation time may increase. These limitation can be overcome using the modified WL transform named S-transform (ST). The S-transform is an invertible time frequency spectral localization technique that combines element of WL transform and short time Fourier transform (STFT) [P. K. Dash, et., al., 2003, S. R. Samantaray, et., al., 2007, Q. Zhang, et., al., 2009, S. Jiao., et., al., 2010, G. Mokryani, et., al., 2010 and A. A. Obed, et., al., 2011].

The main objective of this paper is to develop and implement two approaches to recognize inrush current from faults based on wavelet packet transform (WPT) and S-transform. The MDL criterion is used to select both the mother wavelet and the level of decomposition for the WPT algorithm used. A signatures which represent the values and the time locations of the coefficients depend on the second level details $ad^2$ and $dd^2$ are considered in this algorithm. In the second approach, the spectral energy index and the STD are calculated from the S-matrix and used as an extraction features for signal recognition. The two approaches are examined experimentally on 1KVA, 220/110V, 50Hz, $\Delta / Y$ three-phase transformer and the results revel fast, accurate and reliable methods to recognize different current following in the transformer.

## 2- APPLICATION OF SIGNAL PROCESSING IN DIFFERENTIAL ROTECTION OF POWER TRANSFORMER

The application of signal processing in power system transient has become increasingly popular in recent years due to its effectiveness in capturing short term transients. Basically, STFT transform, wavelet transform and S-transform are a means of obtaining a representation of both time and frequency contents of a differential current signal used in differential protection of power transformer. In this work, a short brief for WPT and ST are given.

### 2.1 Wavelet Packet Transform

Wavelet packet transform is a type of wavelet-based signal processing in a way that each level of resolution (octave) j consists of $2^j$ boxes generated by a tree of low pass filter (LPF) and high pass filter (HPF) operations. The frequency bandwidth of a box decreases with growing octave number i.e. with increasing octave number, the frequency resolution becomes higher while the time resolution is reduced. Starting with a discrete signal f[n] with length $N$, the first level, j=1, decomposition produces two subbands discrete signals $a^1[N/2]$ and $d^1[N/2]$ as follows [G. Stang , et., al., 1996 and M. A. S. K. Khan, et., al., 2007]

$$a^1[n] = \sum_{k=0}^{N-1} g(k)\, f(n-k) \qquad (1)$$

$$d^1[n] = \sum_{k=0}^{N-1} h(k)\, f(n-k) \qquad (2)$$

where $a^1[n]$ and $d^1[n]$ are the first level approximations and details respectively, k is an integer and g(n), h(n) are the LPF and HPF associated with a selected mother wavelet function respectively. The output of both LPF and HPF are downsampled by two at the end of each filtering stage in order to increase the frequency resolution and to ensure the time localization of each frequency subband. The second level of decomposition will produce four subbands due to the decomposition of both $a^1[N/2]$ and $d^1[N/2]$ using the same set of filters. These subbands are $aa^2[N/4]$ $ad^2[N/4]$, $da^2[N/4]$ and $dd^2[N/4]$ as follows

$$aa^2[n] = \sum_{k=0}^{\frac{N}{2}-1} g(k)\; a^1(n-k) \qquad (3)$$

$$ad^2[n] = \sum_{k=0}^{\frac{N}{2}-1} h(k)\; a^1(n-k) \qquad (4)$$

$$da^2[n] = \sum_{k=0}^{\frac{N}{2}-1} g(k)\; d^1(n-k) \qquad (5)$$

$$dd^2[n] = \sum_{k=0}^{\frac{N}{2}-1} h(k)\; d^1(n-k) \qquad (6)$$

A higher level of decomposition can be produced in the same procedure above.

The main advantage of WPT over continuous and discrete wavelet transform is better, more accurate and more detailed representation of the decomposed signals [G. Stang, et., al., 1996]. Also, wavelet packet basis functions are localized in time offering better signal approximation and decomposition. These basis functions are generated from one base function at scale s, dilation $a$ and translation $b$ as follows

$$w_{s,a,b}(n) = 2^{j/2}\, W_a(2^{-j}(n-b)) \qquad (7)$$

where $W_a(n)$ is the wavelet function coefficient matrix. In WPT, a discrete signal $f[n]$ is represented as a sum of orthogonal

Wavelet basis functions $w_{s,a,b}(n)$ as follows:

$$f[n] = \sum_{s}\sum_{a}\sum_{b} w_{s,a,b}[n]\, W_a[n] \qquad (8)$$

The implementation procedure of the WPT for two levels is shown in the decomposition tree of Fig.1.

## 2.2 The Extended Wavelet Transform: S-Transform

The S-transform, is an extension to the ideas of wavelet transform, and is based on a moving and scalable localizing Gaussian window. From the S-matrix, an important information in terms of magnitude, phase and frequency can be extracted. Further, feature extraction is done by applying standard statistical techniques onto the S-matrix.

Many features such as amplitude, variance, mean, standard deviation and energy of the transformed signal are widely used for proper classification. The S-transform is fully convertible from the time domain to two-dimensional (2-D) frequency translation domain and to then familiar Fourier frequency domain. The amplitude frequency- time spectrum and the phase-frequency- time spectrum are both useful in defining local spectral characteristics.

The S- transform produces a time frequency representation of a time varying signal by uniquely combining the frequency depended resolution with simultaneously localizing the real and imaginary spectra. The S-transform is similar to the wavelet transform but with a phase correction and here both the amplitude and phase spectrum of the signal are obtained. Since the S-transform provide the local spectrum of a signal, the time averaging of the local spectrum gives the Fourier transform [P. K. Dash, et., al., 2003 and M. V. Chilukuri, et., al., 2004].

## CONTINUOUS S- TRANSFORM

It is well known that information is contained in the phase of the spectrum, as well as in the amplitude. In order to utilize the information contained in the phase of the continuous wavelet transform (CWT), it is necessary to modify of the mother wavelet. The CWT W(τ, a) of a function f(t) is given as

$$W(\tau, a) = \int_{-\infty}^{\infty} h(t)\; W(t-\tau, a)\, dt \qquad (10)$$

where $W(\tau, a)$ is a scaled replica of the fundamental mother wavelet, the dilation a determines the width of the wavelet and this controls the resolution. The S-transform is obtained by multiplying the CWT with a phase factor as [S. Sendilkumar, et., al., 2009, P. K. Dash, et., al., 2003 and M. V. Chilukuri, et., al., 2004].

$$S(\tau, f) = \exp(i2\pi f\tau).\; W(\tau,\; a) \qquad (11)$$

where f is the frequency, and the quantity $\tau$ is a parameter which controls the position of Gaussian window on the t-axis and a is the dilation factor. The mother wavelet for this particular case is defined as

$$w(t, f) = \frac{|f|}{\sqrt{2\pi}}.\; \exp\left(\frac{-t^2 f^2}{2}\right).\exp(-i2\pi ft) \qquad (12)$$

In the equation above, the dilation factor "a" is the inverse of the frequency f. Thus, the final form of the continuous S-transform is obtained as

$$S(\tau, f) = \int_{-\infty}^{\infty} h(t).\frac{|f|}{\sqrt{2\pi}} \exp\left(\frac{-(\tau-t)^2 f^2}{2}\right).\exp(-i2\pi ft)dt \qquad (13)$$

and the width of the Gaussian window $\sigma(f)$ is

$$\sigma(f) = T = \frac{1}{|f|} \qquad (14)$$

## DISCRETE S-TRANSFORM

The signal h(t) can be expressed in a discrete from as h(kT), k=0,1,…......,N-1 and T is the sampling time interval. The discrete Fourier transform of h(kT) is obtained as [P. K. Dash, et., al., 2003 and M. V. Chilukuri, et., al., 2004]

$$H\left[\frac{n}{NT}\right]=\frac{1}{N}\sum_{k=0}^{N-1}h(kT).\exp\left(\frac{-i2\pi nk}{N}\right) \qquad (15)$$

where n=0, 1,………., N-1. Using eq. (13), the S-Transform of a discrete time series h(kT) is obtained by making $f = n/NT$ and $\tau = jT$ as

$$S\left[jT,\frac{n}{NT}\right]=\sum_{m=0}^{N-1}H\left[\frac{m+n}{NT}\right]G(m,n)\exp(i2\pi mj/N) \qquad (16)$$

and

$$G(m,n)=\exp(-2\pi^2 m^2/n^2) \qquad (17)$$

where j, m =0, 1, 2,….…, N-1, and n= 1, 2,….…, N-1. For n=0

$$S(jT,0)=\frac{1}{N}\sum_{m=0}^{N-1}h\left(\frac{m}{NT}\right) \qquad (18)$$

Equation 18 gives the constant average of the time series into zero frequency, so that the amplitude of the S-matrix over the time results in Fourier spectrum. The amplitude and phase of the S-transform are obtained as

$$\left|S\left[jT,\frac{n}{NT}\right]\right|,\ \tan^{-1}\left\{Imag\left(S\left[jT,\frac{n}{NT}\right]\right)/Real\left(S\left[jT,\frac{n}{jT}\right]\right)\right\}$$

The multiresolution S-transform output is a complex matrix, the row of which is the frequency and the columns are the time values. Each column thus represents the "local spectrum" for that point in time. Also, frequency-time contours which have the same amplitude spectrum are obtained to detect, and localize signal disturbance events. A mesh three-dimensional (3-D) of the S-transform output yields frequency-time, amplitude-time, and frequency-amplitude plots.

## 3. EXPERIMENTAL SETUP AND DATA COLLECTION

The initial and important step in this work is to setup the protected transformer with all necessary equipments to accurately collect the needed data for analytical purpose and then to protect the transformer from internal faults. Figure 2 shows the schematic diagram for the implemented protection system given in Fig.3. The system is applied to 1KVA, 220/110V, 50Hz, $\Delta / Y$ three-phase transformer. Three identical current transformer (CTs) are connected in Y on the $\Delta$ connected primary side while another three identical CTs are connected in $\Delta$ on the Y connected secondary side. The ratios of the primary side CTs and the secondary side CTs are chosen in a manner that guarantees a negligible value of the differential current under steady state operation conditions. The differential current signal of the three phases passes through $1\Omega$ resistor combination. Theses signals are sent into personal computer (PC) through analogue to digital circuit (LabJack-U3-HV), shown in Fig.4. The LabJack can operate also as digital to analogue converter.

The collected data consists of the differential current of different magnetizing inrush current, different external fault currents and different internal current under load and noload conditions. For the case of collecting data, a conductor, timer and switch (switching circuit), as shown in Fig.5, is used to isolate the transformer after ten cycles from the running instant to avoid damage in the transformer and the equipments used.

When the decision features are extracted and the algorithm of WPT and ST are ready to use, the tripping signal, if initiated, is used to isolate the supply by a relay circuit connected instead of the switching circuit. The schematic and the implemented relay circuits are shown in Figs. 6 and 7. The digital trip signal

Generated from the recognition algorithms is converted to analogue by the LabJack and sent

to the relay circuit to use it for the complete system protection.

The data for different operating conditions is sampled at 6.4kHz, 128 samples per cycle and stored to be processed for constructing the features in the two mentioned algorithms.

## 4. DECISIONS FOR EXTRACTION FEATURES

In order to detect any fault following a disturbance, it is necessary to build an extraction features. A successful feature involves the identification of abnormal conditions by the mathematical modeling of the complete system or the analysis of the fault current signature resulting from different transient disturbances. A signature analysis method is used in the two approaches used in this work.

### 4.1. WPT Approach

Three various conditions from the collected data are used for the analysis of selecting the optimal mother wavelet filter and the number of level of decomposition. These various conditions are; unloaded magnetizing inrush current, primary double line to ground internal fault loaded and single line to ground external fault loaded.

The optimal mother wavelet filter can be selected by calculating the MDL index using the following formula [N. Saito, 1994 and S. A. Saleh, et. al., 2005]

$$MDL_x(k,j) = \min\left\{\frac{3}{2}k\log N + \frac{N}{2}\log\left\|\bar{\alpha}_{xj} - \bar{\alpha}_{xj}^{(k)}\right\|^2\right\} \quad (19)$$

Where $0 \le k < N$ which represents the length of the signal $f[n]$, $1 \le j < M$ the total number of wavelet filter (level of resolution) used for the decomposition of the signal $f[n]$, $\bar{\alpha}_{xj} = W_{xj}f[n]$ denotes to the vector of decomposition coefficients of $f[n]$ up to level $j$, $\bar{\alpha}_{xj}^{(k)} = \theta^{(k)}W_{xj}f[n]$ denotes to the vector that contains $k$ non-zero elements and $\theta^{(k)}$ is the hard threshold operation that keeps the $k$ largest elements of $\bar{\alpha}_{xj}$ in absolute value intact and set all other elements to zero. The first term of the MDL criteria index represents the penalty function that is increasing linearly with the number of the retained wavelet coefficients $k$, while the second term describes the logarithmic energy residual between $\bar{\alpha}_{x,j}$ and $\bar{\alpha}_{x,j}^{(k)}$. It should be noted that the residual energy decreases as $k$ increases. The number of coefficients k for which the MDL function reaches the minimum value, is considered as an optimal one.

The MDL index is calculated up to the second level of decomposition for five types of orthogonal and bi-orthogonal mother wavelet functions. The results for the three conditions are given in Tables 1, 2 and 3. From the these tables, it can be noted that Daubechies (db4) has the smallest value of MDL index in the first level. Therefore it can be considered the optimal mother wavelet function. These low values of MDL(1) may be due to the jumps of the data at the switching instant and some missing data. Thus, MDL(1) may not provide accurate indication and the higher levels of resolution will include more detailed representation of the signal. The optimal level of decomposition $j$ is reached when MDL($j$) is less than levels of higher $j$. Table 4 presents four levels of MDL index using db4 mother wavelet. The second level has the lowest values of MDL index. Therefore, the second level is selected as the optimal level of decomposition.

To extract features for the WPT algorithm, the signals of the different differential currents are decomposed up to the second level of resolution by WPT using the selected mother wavelet function (db4). [S. A. Saleh, et. al., 2005] proposes an algorithm for the same features depends on the second level high frequency details ($dd^2$). This approach looks at the second level high and low frequency details ($dd^2$ and $ad^2$) for different current signals. These details are given in Fig. 8.

The values of these coefficients and their time locations represent the needed signatures to recognize the type of the investigated current. It is clear that the normal (inrush) current and the external fault current do not have any high frequency details components in the second level $dd^2$ and a threshold value for low frequency details in the second level. When an internal fault occurred, the details $dd^2$ and $ad^2$ show a threshold value frequency components, which can be used as a features extraction recognition. Therefore, the WPT algorithm is depended on the identification of $dd^2$ and $ad^2$ components or coefficients in the second level.

**4.2 S-Transform Approach**

The computation of the discrete S-transform can be outlined as follows.

1. Denote n/NT, m/NT, kT, and jT as n, m, k, and j respectively, for all of the computations.
2. Obtain discrete Fourier transform H[n] of the original time-varying signal h[k], with N points and sample interval T, using DFT routine from eq. (15).
3. Compute the localizing Gaussian G[n,m] for the required frequency n using eq. (17).
4. Shift the spectrum H[n] to H[m+n] for the frequency n by using convolution theorem.
5. Obtain the product of H(m+n) and G(m+n) and take inverse Fourier transform of the product to get S transform as eq. (16).

The multiresolution S-transform output is a complex matrix, the row of which is the frequency and the columns are the time values. Each column thus represents the "local spectrum" for that point in time. Also, frequency-time contours which have the same amplitude spectrum are obtained to detect, and localize signal disturbance events. A mesh three-dimensional (3-D) of the S-transform output yields frequency-time, amplitude-time, and frequency- amplitude plots.

To illustrate the use of multiresolution S-transform for nonstationary signal analysis, a sample of inrush current waveform in a data window of eight cycles (using a sampling rate of 128 samples/ cycle) is considered. The three-dimensional (3-D) mesh for the signal shown in Fig. 9(a) is shown in Fig. 9(b). From the 3-D plot, one can find the magnitude, frequency, and time information's to detect, localize, and visually classify the event. Also, it is observed that the increase or decrease of the signal magnitude can be deduced from the innermost (or the lowest level) contour. Similar plots are shown for a sample of internal fault current waveform in Fig. 10. It is mentioned here that the time axis is replaced by the number of samples.

After the signal is retrieved, S-transform is used to process the signal samples to provide the relevant features for identifying the type of fault. The energy of inrush current and fault current are computed through Parseval's theorem [M. O. Oliveira, et., Al., 2008] from S-matrix output. On the other hand, the standard deviation is directly applied to the S-matrix output to derive the Standard Deviation (STD) values for the corresponding phase, for example, the feature extraction of energy and standard deviation of S-transform contour are obtained from Matlab functions as [S. Sendilkumar, et., al., 2009]

Energy a = (S-matrix a) ^ 2 (20)
S-matrix a = S-matrix of phase a and
STD a = std (abs (S-matrix a)) (21)

Table 5 shows the spectral energy and the STD for different inrush, internal and external fault current for different connections of the three-phase transformer. It can be seen from this table that the values of energy vector and STD are able to be differentiable effectively between them or as pattern recognition to discriminate between inrush, external and internal fault current. This pattern is used to

Implement the S-transform algorithm used in this work.

## 5. ALGORITHMS IMPLEMENTATION AND EXPERIMENTAL RESULTS

The two algorithms are implemented experimentally to examine the ability of recognition between the internal fault currents and the current of inrush and external faults. Figure 11 shows the flowcharts for the software implementation of the two algorithms. In WPT algorithm, the three-phase differential current is read through the CTs and root summed squared together into one value before being passed to low and high pass filters to construct the first level $d^1$ and $a^1$. The output is downloaded by two and then passed through another low and high pass filter to construct $dd^2$ and $ad^2$. If the absolute value of $dd^2$ and $ad^2$ are higher than threshold, then it generates a trip signal in order to disconnect the transformer from the supply.

In ST algorithm, the S-matrix is calculated for each phase current. The energy and the standard deviation are also calculated. If E and STD are greater than the threshold, then a trip signal is initiated. Otherwise, a restrain signal is appear.

Several magnetizing inrush currents, external and internal fault currents both in load and noload cases are used to test the two algorithm with the hardware of the complete protection system. Three cases differ from that used in MDL calculation. Figure 12 shows the three-phase differential current and the trip signal generated by WPT algorithm (Fig. 12 a) and by ST algorithm (Fig. 12 b) for the case of magnetizing inrush current with a balanced Y-connected full load unity power factor. The two algorithms used do not generate any trip signal. Figure13 shows the same results for the case of loaded external three-phase to ground fault current after energization. The trip signal status is also not changed.

Two cases of different internal faults are considered to show the ability of disconnecting the transformer from the supply. Figures 14 and 15 show the results unloaded secondary three-phase to ground fault and unloaded secondary internal two-phase to ground fault respectively. In the two cases, the trip signal is generated

## 6. CONCULSIONS

This paper presents and applies two approaches for differential protection of power transformer based on WPT and S transforms. The main function of these approaches is how to recognize between (internal faults) and (inrush and external faults). The two approaches do not need any kind of training or harmonic analysis. The WPT method must select the optimal for both the mother wavelet filter and the number level of resolution. This limitation is overcome using S-transform but WPT is fast for recognition of current type. The two methods are quite simple to implement and easy to be coded with a small amount memory for storage and compilation. The two methods are applied with hardware implementation of the overall system and the experimental results are accurate, prompt and can be used for differential protection of power transformer.

## 7- REFERENCES

A. L. Oville-Fernandez, N. K. J. Ghonaim, and J. A. Valencia, “A FIRANN as a Differential Relay for Three Phase Power Transformer Protection”, IEEE Trans. Power Delivery, Vol.16, No. 2, PP. 215-218, 2001.

A. Rahmati “An Adaptive Differential Relay for CT Saturation Based on Wavelet Transform” IEEE, PES T&D, PP1-6, 2010.

A. A. Obed, M. A. Alwan and W. N. Taboor, “A Wavelet Packet Transform-Based Technique for the Discrimination of Inrush Currents from Faults in Three-Phase Transformer” Journal of Basrah Researches, Vol. 37, No. 4A/15, PP 1-14, Aug. 2011.

A.Wiszniewski and B. Kasztenny, “A multi criteria differential transformer relay based on fuzzy logic, IEEE Trans.Power Delivery, 10 (4), 1786-1792, 1995.

B. A. Sykes and I. F. Morrison, “A Proposed Method of Harmonic Restraint Differential

Protection of Transformers by Digital Computer," IEEE Trans. Power App. Syst. vol. PAS-91, pp. 1266-1272, May 1972.

G. Stang and T. Nguyen, "Wavelet and Filter Banks" Wellesley, MA: Wellesley-Cambridge, 1996.

G. Mokryani, M. R. Haghifam, H. Latafat , P. Aliparast, and A. Abdollahy, "Detection of Inrush Current Using S-Transform and Probabilistic Neural Network", Transmission and Distribution conference and Exposition, pp.1-6, IEEE PES, 2010.

H. Khorashadi, "Fuzzy-Neuro Approach to Investigating Transformer Inrush Current," Transmission and Distribution Conference and Exhibition, pp. 1302-1306, May, 2006.

L. D. Periz, A. J. Flechsig, J. L. Mendor, and Z Obradovic, " Training of Artifical Neural Network to Discriminate between Magnetizing Inrush and Internal Faults", IEEE Trans. Power Delivery, Vol. 9, No. 1, PP.434-441, 1994.

M. R. Zaman, "Artificial Neural Network Based Protection of Power Transformer", Ph.D thesis, Memorial University of Newfoundland, St. John's, NF, Canda, 1996

M. V. Chilukuri and P. K. Dash, "Multiesolution S-Transform-Based Fuzzy Recognition System for Power Quality Events" IEEE Tran. Power Delivery., Vol. 19, No. 1, pp.323-330, January, 2004.

M. A. S. K. Khan, T. S. Radwan and M. A. Rahman, "Real Time Implementation of Wavelet Packet Transform Based Diagnosis and Protection of Three-Phase Induction Motors" IEEE Trans. Energy Conversion, Vol. 22, No. 3, Sep., 2007.

M.C.Shin, C.W.Park and J.H.Kim, "Fuzzy Logic - Based Relaying for Large Power Transformer Protection", IEEE Trans.Power Delivery, 18 (3), 718-724, 2003.

M. O. Oliveira, R. H. Salim and A.S. Bretas, "Wavelet Transform Approach for Differential Protection of Three-Phase Transformers", 2008 43rd International universities power Engineering conference, pp.1-5, 2008.

N. Saito, "Simultaneous Noise Suppression and Signal Compression using a Library of Orthogonal Basis and the Minimum Description Length Criterion" in Wavelet in Geophysics. E. Foufoula-Georgiou and Kumar, Eds. New York: Academic, PP. 299-324, 1994

P. K. Dash, B. K. Panigrahi, and G. Panda "Power Quality Analysis Using S-Transform" IEEE Tran. Power Delivery., vol. 18, No. 2,pp.406-411, April 2003

Q. Zhang, S. Jiao and S. Wang, "Identification Inrush Current and Internal Faults of Transformer Based on Hyperbolic S-transform", IEEE Conference on Industrial Electronics and Applications, pp. 258-263, 2009.

S. A. Saleh and M. A. Rahman, "Modeling and Protection of a Three-Phase Power Transformer using Wavelet Packet Transform", IEEE Trans. Power Del., Vol. 20, No. 2, pp. 1273–1282, Apr. 2005.

S. R. Samantaray, B. K. Panigrahi, P. K. Dash and G. Panda, "Power Transformer Protection using S-transform with Complex Window and Pattern Recognition Approach" IET Gener. Transm. Distrib., pp. 278–286, 2007.

S. A. M. Salah and M. A. Rahman "Testing of a Wavelet-Packet-Transform-Based Differential Protection for Resistance-Grounded Three-Phase Transformers" IEEE Trans. On Industry Applications, Vol. 46, No. 3, pp.1109-1117, May/June 2010.

S. A. Saleh, B. Scaplen, and M. A. Rahman, "A New Implementation Method of Wavelet-Packet-Transform Differential Protection for Power Transformers", IEEE Trans. Industry Application., Vol. 47, No. 2, March/April 2011.

S. Jiao and H. Huang, "Research on Identification Between Inrush Current and Internal Faults of Power Transformer Based on H-S Transform," 3rd International congress on Image and signal processing, pp. 3619-3624,2010.

S. Sendilkumar, B. L. Mathur and Joseph Henry, “A New Technique To Classify Transient Events in Power Transformer Differential Protection Using S-Transform” Third International Conference on Power Systems, Kharagpur, INDIA December 27-29, 2009.

**LIST OF SYMBOLS AND APPREVIATIONS**

ANN: Artificial Neural Network
CT: Current Transformer
CWT: Continuous Wavelet Transform
db: Daubechies mother wavelet
DFT: Discrete Fourier Transform
G(m,n): Gaussian Function
$H\left[\frac{n}{NT}\right]$: discrete Fourier transform function
HPF: High Pass Filter
I: current
LPF: Low Pass Filter
KVA: Kilo Volt Amper
MDL: Minimum Description Length
PC: Personal Computer
R: Relay
$S\left[jT, \frac{n}{NT}\right]$: S transform function of the discrete signal
$S(\tau, f)$: S transform function of the continuous signal
ST : S Transform
STD: STandard Deviation
STFT: Short Time Fourier Transform
WL: WaveLet
WPT: Wavelet Packet Transform
$W(\tau, a)$ : continuous wavelet transform function

$\alpha_N$ : vector of the decomposition coefficients of f
$\alpha_N^{(k)}$ : vector of the continuous nonzero elements
$\theta^{(k)}$ : hard-threshold
$\sigma(f)$ : Gaussian window

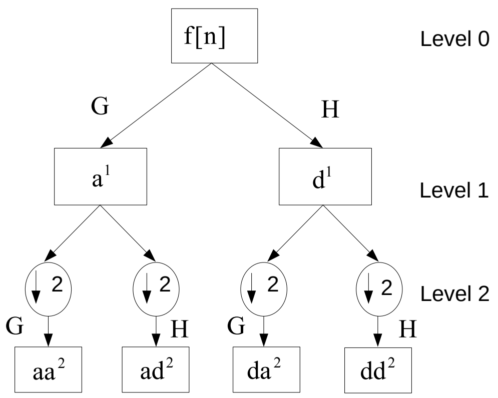


**Fig.1 Two levels of decomposition by WPT**

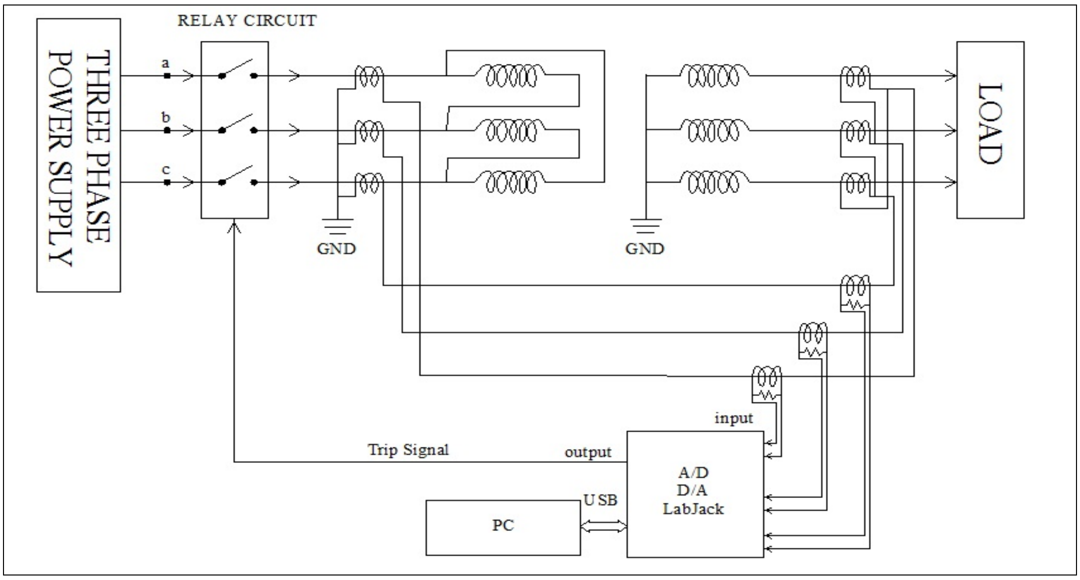


**Fig.2 Schematic diagram for differential protection of the three- phase power transformer**

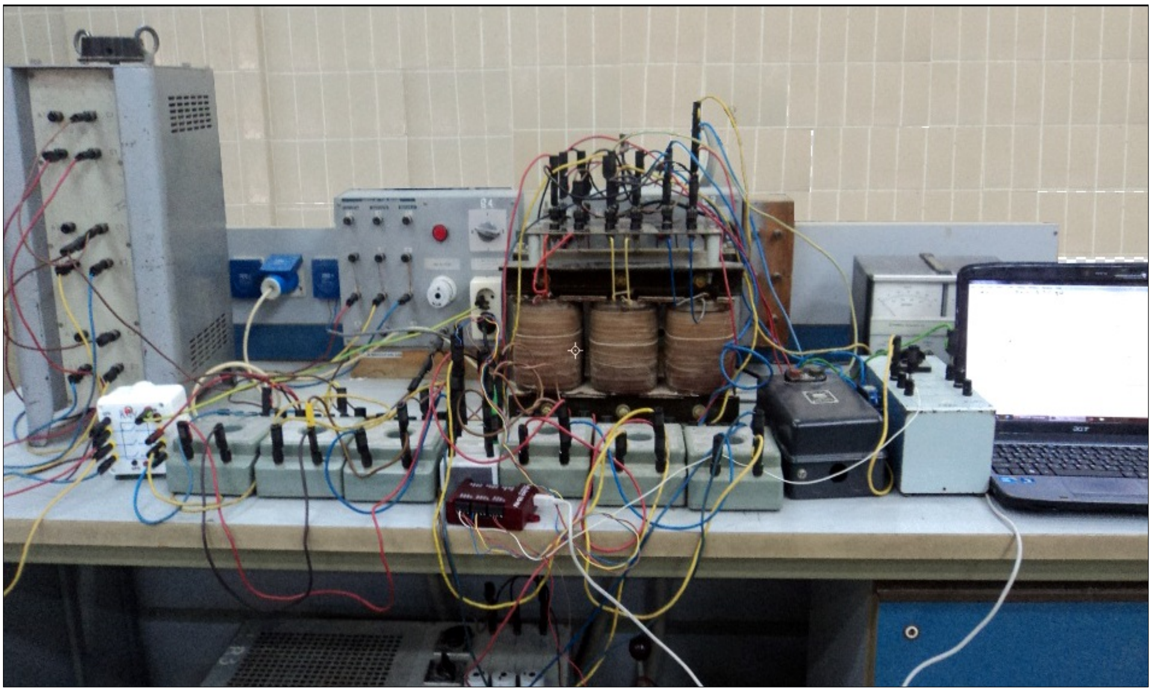

**Fig.3 Implemented system for differential protection of the three- phase power transformer**

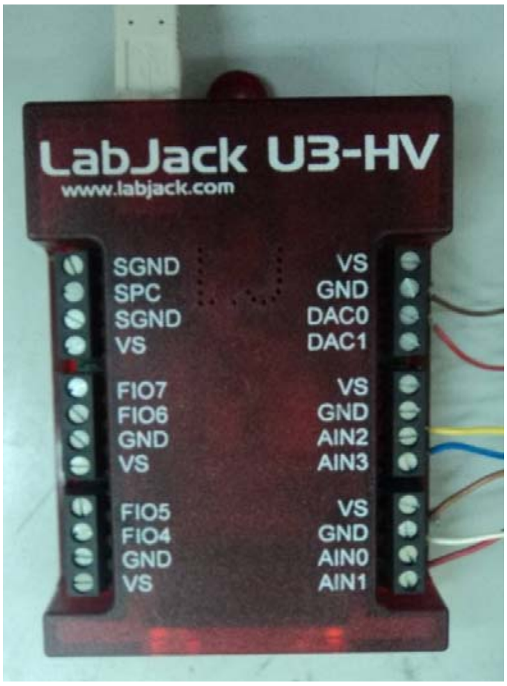


**Fig.4 (Lab Jack U3-HV) circuit**


**Fig. 5 The switching circuit**

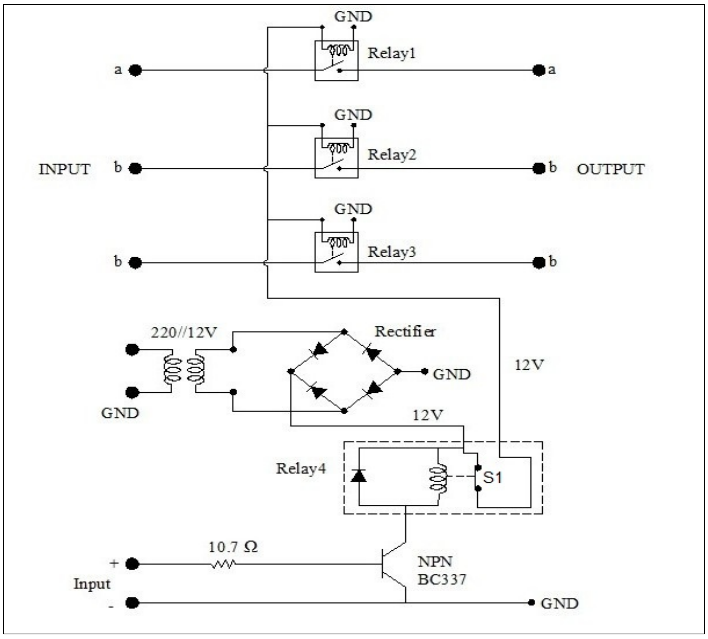


**Fig. 6 Schematic diagram of relay circuit Circuit**

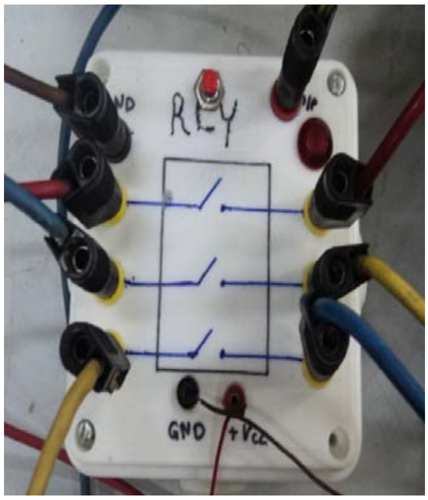


**Fig.7 The implemented relay**

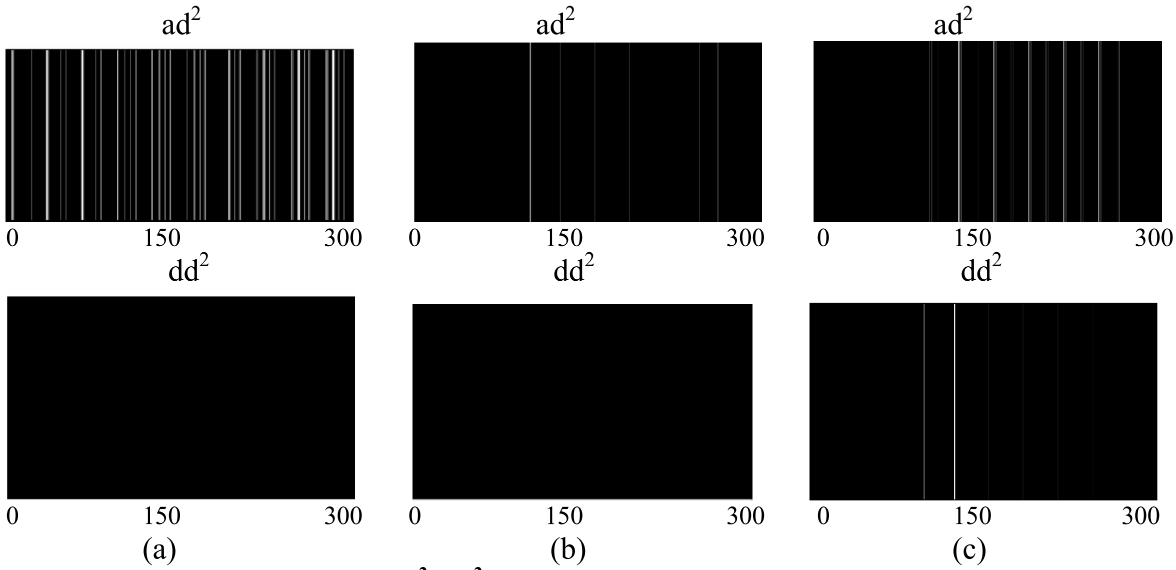


**Fig. 8 Second level coefficients $ad^2$, $dd^2$, (a) inrush current, (b) external fault, (c) internal fault.**

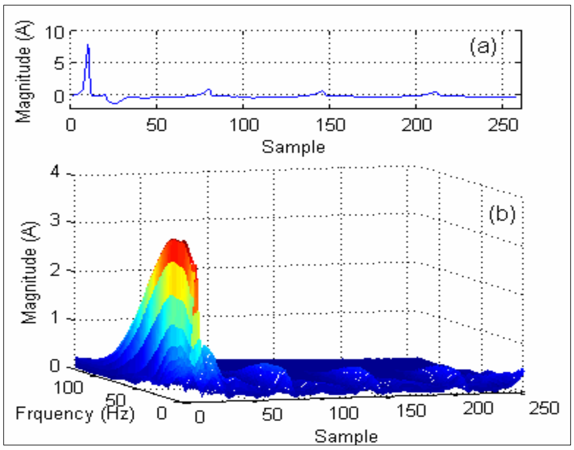


**Fig. 9: (a) Inrush current (b) 3-D S-Transform plot**

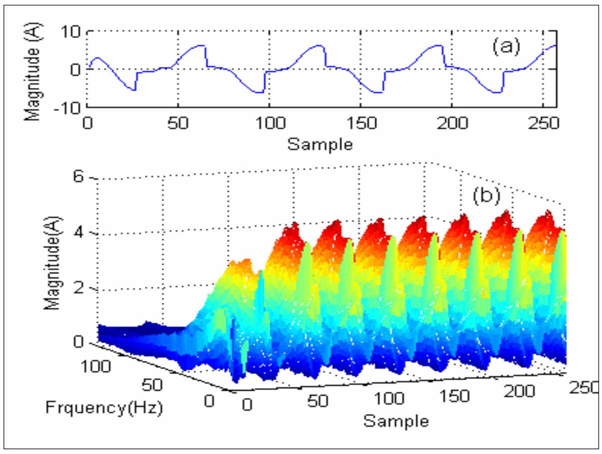


**Fig. 10 (a) Internal fault current (b) 3-D S transform**

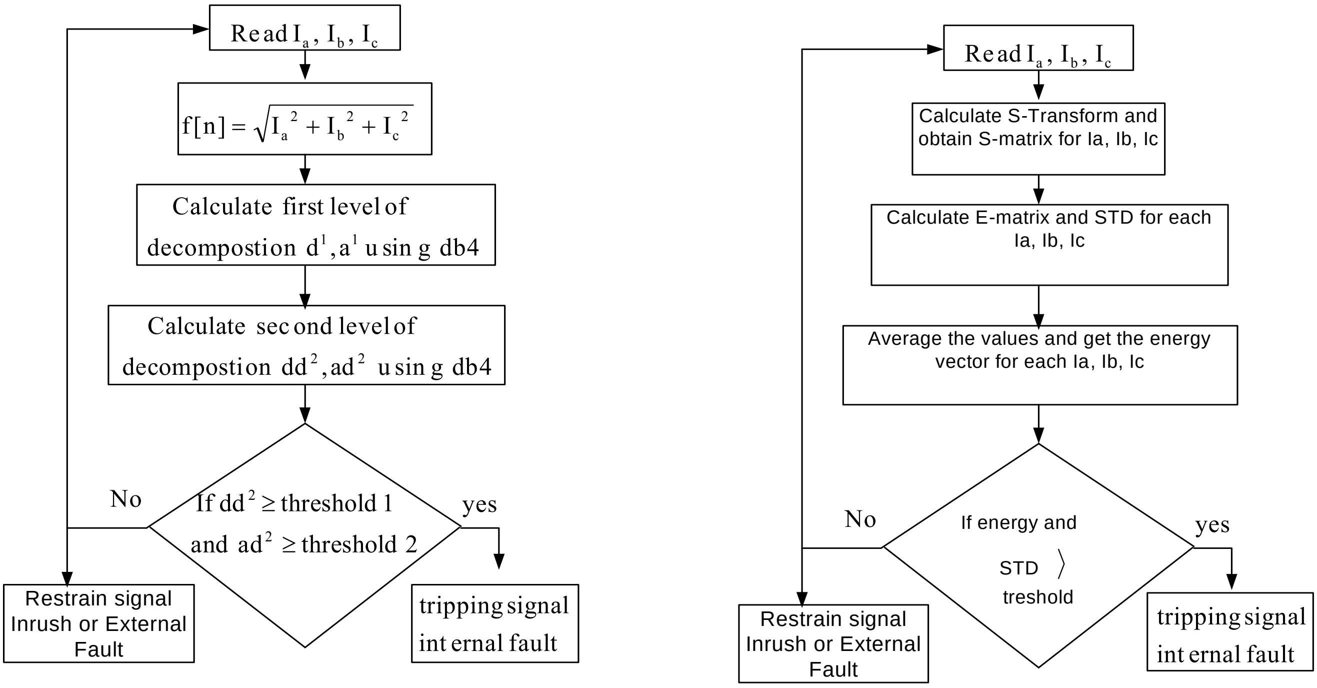


(a) (b)

**Fig. 11 Flowchart for software implementation for (a) WPT algorithm (b) ST algorithm**

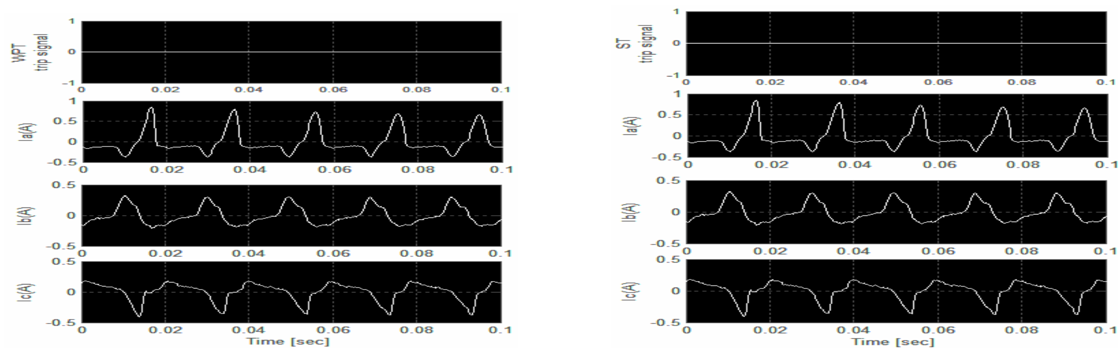


(a) (a)

**Fig.12 Three-phase differential current and the trip signal for the case of loaded inrush current before energization (a) by WPT algorithm, (b) by ST algorithm**

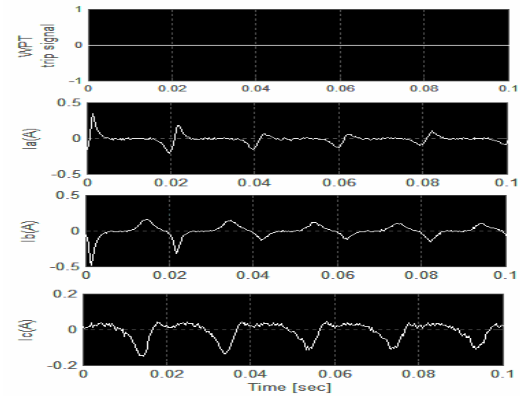


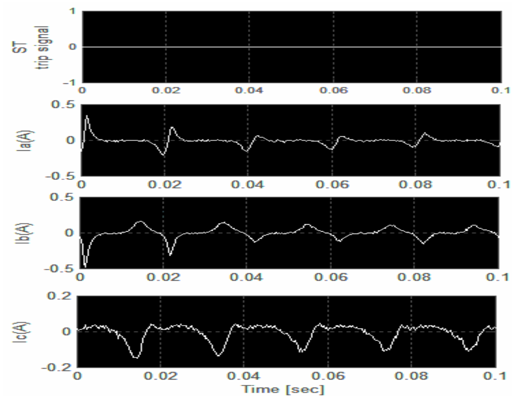


(a) (b)

**Fig.13 Three-phase differential current and the trip signal for loaded external 3-ph to ground fault current after energization (a) by WPT algorithm (b) by ST algorithm.**

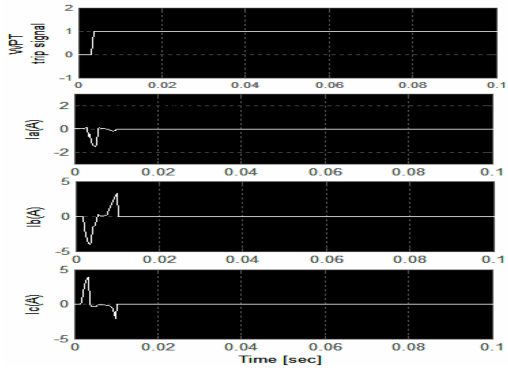


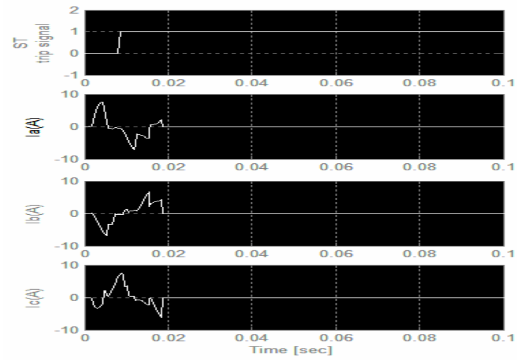


(a) (b)

**Fig.14 Three-phase differential current and trip signal for secondary unloaded internal 3-ph to ground fault after energization (a) by WPT algorithm (b) by ST Algorithm**

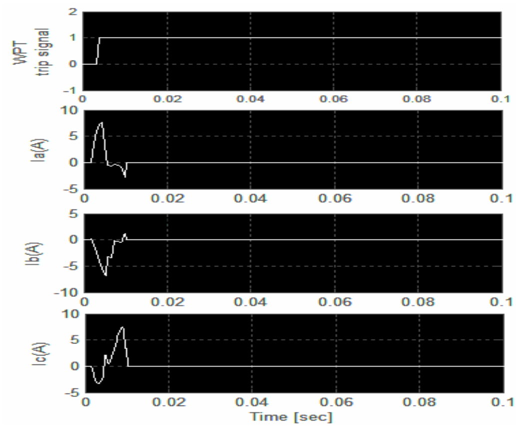


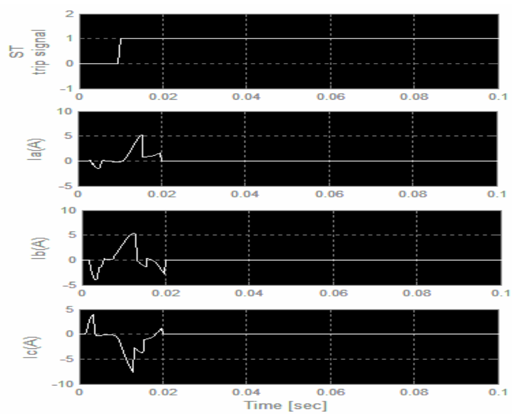


(a) (b)

**Fig. 15 Three-phase differential current and trip signal for unloaded secondary internal two-phase to ground fault (a) by WPT algorithm (b) by ST Algorithm**

**Table 1, MDL index for inrush current**

| Mother Wavelet | MDL(1) | MDL(2) |
|---|---|---|
| db4 | 1.5399 | 0.9865 |
| coif1 | 5.68 | 4.7957 |
| sym2 | 20.8061 | 1.8741 |
| bior1.1 | 112.7782 | 11.1746 |
| db10 | 10.1095 | 7.5879 |

**Table 2. MDL index for internal fault**

| Mother Wavelet | MDL(1) | MDL(2) |
|---|---|---|
| db4 | 3.3744 | 1.0476 |
| coif1 | 70.7034 | 7.8594 |
| sym2 | 62.5534 | 0.1653 |
| bior1.1 | 174.3035 | 38.151 |
| db10 | 4.592 | 3.3369 |

**Table 3, MDL index for external fault**

| Mother Wavelet | MDL(1) | MDL(2) |
|---|---|---|
| db4 | 3.1112 | 0.6934 |
| coif1 | 6.0301 | 4.4436 |
| sym2 | 15.4894 | 0.2691 |
| bior1.1 | 184.4074 | 2.0319 |
| db10 | 6.345 | 3.465 |

**Table 4, Four levels MDL index**

| Current data | MDL(1) | MDL(2) | MDL(3) | MDL(4) |
|---|---|---|---|---|
| Unloaded inrush | 1.5399 | 0.9865 | 2.3746 | 1.8191 |
| Primary DLG fault | 3.3744 | 1.0476 | 1.7611 | 1.8733 |
| External SLG fault | 3.1112 | 0.6934 | 2.5005 | 1.7593 |

**Table 5 Energy and standard deviation for inrush and fault currents**

| INRUSH /FAULT | ENERGY | STD |
|---|---|---|
| **Inrush loaded** | | |
| Inrush-a-(Δ-Y) | 0.0091 | 0.0203 |
| Inrush-b-(Δ-Y) | 0.0024 | 0.0055 |
| Inrush-c-(Δ-Y) | 0.0025 | 0.0056 |
| **Internal Fault** | | |
| Fault Δ-Y bc-g(b) | 0.8197 | 1.7759 |
| Fault Δ-Y bc-g(c) | 0.8608 | 1.92333 |
| Fault Δ-Y abc-g(a) | 1.0967 | 2.3607 |
| Fault Δ-Y abc-g(b) | 1.1464 | 2.4688 |
| Fault Δ-Y abc-g(c) | 0.8596 | 1.8503 |
| **External Fault** | | |
| Fault Δ-Y abc (a) | $2.9049*10^{-4}$ | $6.5615*10^{-4}$ |
| Fault Δ-Y abc (b) | $8.5276*10^{-4}$ | $1.8751*10^{-3}$ |
| Fault Δ-Y abc (c) | $2.9049*10^{-4}$ | $6.5615*10^{-4}$ |